Journal of Cereal Science 87 (2019) 25–30

Contents lists available at ScienceDirect

Journal of Cereal Science

journal homepage: www.elsevier.com/locate/jcs

Raman and Fourier transform infrared spectroscopy application to the Puno and Titicaca cvs. of quinoa seed microstructure and perisperm characterization

Borisz Czekus[a], Ilinka Pećinar[b], Ivana Petrović[b], Novica Paunović[c], Slađana Savić[a,*], Zorica Jovanović[b], Radmila Stikić[b]

[a] Faculty of Biofarming, Megatrend University, Bulevar maršala Tolbuhina 8, 11070 Belgrade, Serbia
[b] Faculty of Agriculture, University of Belgrade, Nemanjina 6, 11080 Belgrade, Serbia
[c] Institute of Physics, University of Belgrade, Pregrevica 118, 11080 Belgrade, Serbia

ARTICLE INFO

Keywords:
Quinoa
Seed anatomy
Composition
Raman
FT-IR

ABSTRACT

The aim of this study was to investigate the quinoa fruit and seed microstructure, as well as to determine the qualitative composition of quinoa whole seed spatial localisation of food reserves in cultivars Puno and Titicaca using two complementary spectroscopic techniques (Fourier Transform infrared and Raman). The analyses of the seeds also included measurements of the crude proteins and starch contents. The experiment was carried out during the 2016 growing season in rain-fed conditions in the north of Serbia. The analysis of the scores of the principal components based on the Raman spectra revealed two groups in both seed parts (cotyledons and perisperm). The analysis of the loadings highlighted the spectrum region that contributed to the differentiation, e.g. the band at 472 cm^{-1} was related to the amylopectin content in the perisperm region. As for the cotyledons, the spectral range from 1100 to 1650 cm^{-1} was responsible for genotype differences and it included both the most important bands derived from Amide I, II and quinoa protein with globoid crystals composed of phytin. IR analysis, similar to the analyses of the crude proteins and starch contents in the seeds, failed to reveal any differences in biochemical composition between two analyzed genotypes.

1. Introduction

Quinoa (*Chenopodium quinoa* Willd.) is a pseudo-cereal crop belonging to the Amaranthaceae family and originated from South America. It is an annual plant, and currently is in focus due to its high tolerance to various stress factors including frost, drought, salinity (Jacobsen and Muica, 2002), as well as its exceptional nutritional value of seeds and certain vegetative parts of the plants (Gordillo-Bastidas et al., 2016). The storage reserves of proteins, mineral nutrients, and lipids in the seeds are mainly located in the reduced endosperm and the cotyledons (Valencia-Chamorro, 2003), while carbohydrate reserves are found in the perisperm, nominated as seed storage tissues (Prego et al., 1998). The nutritional value is also based on the substantial fiber and protein contents which are higher in comparison to these contents found in corn and rice. On the other hands, these contents are similar those recorded in wheat (Gordillo-Bastidas et al., 2016). The major protein fractions are albumins and globulins. They account for 77% of protein in total, whose biological value is comparable to casein. On the other hand, the specific content of amino acids comes from lysine, histidine and a high level of sulfur containing amino acids (cysteine and methionine) (Gordillo-Bastidas et al., 2016).

Most of the information on the structural features of quinoa fruit and seed to date has been found in studies conducted by Varriano Marston and DeFrancisco (1984), Prego et al. (1998), Sukhorukov and Zhang (2013). Raman microspectroscopy is currently used as a highly powerful and useful tool for the rapid evaluation of seed composition. The advantages of Raman are as follows: this technique is non-destructive, very fast and sensitive; the samples can be analyzed directly without any staining and complicated sample preparation, and at the same time the chemical and structural information can be gained in the native state. Previous studies demonstrated the successful application of Raman spectroscopy in starch analysis in different grains (Kizil et al., 2002; Almeida et al., 2010), as well as proteins in soybean seed (Lee et al., 2013) and phytin in wheat grain (Kolozsvari et al., 2015). However, Raman technique has not yet been used for analyses of quinoa seeds.

* Corresponding author.
E-mail address: bonita.sladja@gmail.com (S. Savić).

https://doi.org/10.1016/j.jcs.2019.02.011
Received 29 October 2018; Received in revised form 25 February 2019; Accepted 26 February 2019
Available online 27 February 2019

Another technique, infrared spectroscopy is a useful tool which provides efficient information of sample composition. It reveals structural components of biological samples based on the specific molecular vibrations and exposes the unique spectral fingerprint of the analyzed object. It is used for analysis of food and other agricultural crops. According to the literature, the quinoa seed was previously analyzed by NIR - near infrared spectroscopy (Encina-Zelada et al., 2017). Similarly, quinoa flour was analyzed by FT-IR and this methodology is recognized as a relevant analytical tool for the determination of flour composition (Rossell, 2013; Garcia-Salcedo et al., 2018). Rossell (2013) showed that a portable FTIR system can be used for detection of quinoa flour authenticity. Out of 45 of different flour samples, quinoa flour was separated by carbohydrate stretching (C—C and C—O bonds) and deformation (C—O—C) spectral signals in the 950-1000 cm^{-1} region. In addition, the amide region at 1560-1665 cm^{-1} was detected as a reliable region for flour differentiation (Rossell, 2013).

The nutritional and health promoting values of the seeds together with stress resistance properties of the quinoa plant make it attractive for numerous countries, especially for those facing the effects of climate change on their food production and food security. United Nations Food and Agriculture Organization (FAO) selected quinoa as one of the crop destined to offer food security in the 21st century and declared 2013 as the International Year of Quinoa (www.fao.org/quinoa-2013/en/). However, although the southern Europe is already faced with climate changes reducing effects on agricultural production, cultivation of quinoa is still limited, except for Italy and Greece (Pulvento et al., 2015; Noulas et al., 2015). In Serbia, as a country with the southeastern European agro-climatic conditions, quinoa has not yet been grown. Preliminary research of Stikic et al. (2012) confirmed good seed nutrient quality, with high protein content and content of mineral and most essential amino acids (especially lysine) when quinoa Danish cultivar Puno (Jacobsen and Muica, 2002) was grown in Serbian rain-fed field conditions.

The aim of the present study was to assess the macro and microstructure of quinoa fruit and to apply Raman and FTIR spectroscopy for determination of seed quantitative composition of two quinoa cultivars Puno and Titicaca. Since the trial was done in Serbian agro-climatological conditions, it is expected that the results would help to introduce the cultivation of quinoa, as an alternative crop, in Serbia.

2. Material and methods

2.1. Source of plant material and measurements

The experiment was carried out during the 2016 growing season in rain-fed conditions using two introduced genotypes of quinoa adapted to the European climate, Puno and Titicaca, selected at the University of Life Sciences in Copenhagen, Denmark (Jacobsen and Muica, 2002). The quinoa was grown on a small Serbian farm near Subotica and in the area between the north latitudes of 46° and east longitudes of 19.68° (about 10 km south from the Serbian and Hungarian border). The soil type was chernozem, medium rich in nitrogen (0.24%) and hummus (3.19%), highly rich in phosphorus (34.68 mg P_2O_5/100 g soil) and rich in potassium (29.42 mg K_2O/100 g soil), slightly alkaline (pH 7.66). The seeds were sowed in the first part of April, when the soil temperature reached 12 °C. The experiment was laid out in a split-split plot system, with four replications. The size of the main plot was 12 m^2. The distance between the rows was 50 cm and between the plants in the row −5 cm (approximately 400 000 seeds per hectare). The seeds were sown at a depth of 2 cm. No fertilizer was applied during the vegetative season. The crops were harvested in the first half of August when quinoa fruits/seeds were ripeness, the moisture content was 12%. During vegetation, there was a 40-day period with the maximum air temperature of over 30 °C, which suited this thermophile plant. The temperature data was obtained from the automatic meteorological station located in the center of Subotica, at a 4-km distance from the experimental field. The measurements were collected using “Nexus” instruments and “Weather Display” software (http://www.sumeteo.info). The amount of precipitation was measured on site, at the experimental field. Over the five months of vegetation, there were 22 days with precipitation. The overall amount of precipitation before harvest was 317 mm. At physiological maturity, the harvest of Puno and Titicaca seeds was made by hand. The seeds were ground by using a laboratory mill (model Cemotek Sample Mill Foss, Sweden) and then the contents of proteins and starch were analyzed. The content of crude proteins was determined according to Kjeldahl method (Stikic et al., 2012), while for starch measurement the Ewers polarimetric method was used (ISO and 10520: 1997). Two complementary spectroscopic techniques (Fourier Transform infrared and Raman) were carried out for the analyses of Puno and Titicaca seeds and fruits microstructure and composition.

2.2. Light microscopy

Dry fruit materials of *Ch. quinoa* genotypes were studied using light microscopy. The bright field light microscope in reflected light (Stereomicroscope Nikon SMZ18, Tokyo, Japan) was used at a magnification up to 20x. Images were acquired using a Nikon DIGITAL SIGHT DS-Fi1c digital camera. In addition, longitudinal sections of the *Ch. quinoa* seeds were observed by brightfield light microscopy in transmitted light (Leica DM2000, Germany), and documented with a Leica DC320 digital camera, and a Leica IM1000 software was used for sample capture.

2.2.1. Specimen preparation for light microscopy

For microstructure studies, fruit samples were fixed in 50% ethanol. Dehydration of fixed tissue samples was performed in a LEICA TP1020-Automatic Tissue Processor through a gradual series of ethanol (80%, 96% and absolute ethyl alcohol) and the xylene and melted paraffin embedding medium (Histowax, 56–58 °C). Tissues were embedded using an EG1120 Paraffin Dispenser with an integrated hot plate. After cooling and hardening of the paraffin blocks on the Leica EG1130 cold plate, transverse sections (thickness 5–10 μm) were cut on a LEICA SM 2000 R microtome. Paraffin was removed from the sections using a deparaffinisation procedure of passing through a series of ethyl alcohol solutions (absolute, 95%, 70%, 50% and 30%) and the tissue was stained in safranin (overnight) and alcian blue (for a duration of 2s). After staining, the tissue was dehydrated rapidly through absolute alcohol and xylol. Deparaffinisation, staining and dehydratation of microslides were conducted using a LEICA ST4040 Linear stainer. Finally, slides were mounted in Canada balsam for microscopic examination.

2.3. Raman instrumentation

Raman spectroscopy was performed using a XploRA Raman spectrometer from Horiba Jobin Yvon on the longitudinal fruit section samples. The Raman scattering was excited by a frequency-doubled Nd/YAG laser at a wavelength of 785 nm (maximum output power 20–25 mW) equipped with a 600 lines/mm grating. Spectra were accumulated from 5 scans, during 10s and filter 100%. In order to take into account any sample inhomogeneity, at least ten Raman spectra were recorded for each sample and for two parts of seed (cotyledon and perisperm) using single point Raman measurements at 50x objective lens. The spectra were recorded in the range between 200 and 1600 cm^{-1} in the perisperm region and from 250 to 1750 in the cotyledon region. All recorded measurements were with 4 cm^{-1} spectral resolution. The Raman spectra acquisitions were managed by the LabSpec software (Horiba Jobin Yvon).

2.4. FT-IR instrumentation

The IR transmission measurements were performed at room

temperature with the Nicolet Nexus 470 Fourier-transform IR spectrometer. The KBr beamsplitter and the DTGS detector were used to cover the wavenumber range between 600 and 4000 cm^{-1}. The transmission spectra were recorded with the resolution of 2 cm^{-1} and with 256 interferometer scans added for each spectrum. The samples were prepared for the IR spectra measurements by grinding the seeds in liquid nitrogen and mixing it with the KBr powder. The mixture was further pressed into tablets under the conditions outlined above.

The characteristic bands of the specific functional groups were described from the literature records. Raman and FT-IR spectra were analyzed by the OriginPro 8.6 software (OriginLab, Northampton, MA, USA).

2.5. Chemometric analysis of the Raman spectroscopic data

For all PCA analyses, the data were preprocessed, *i.e.* the Raman spectra were smoothed using Savitzky-Golay filters with 4 points and a second-order polynomial function. All Raman scattering intensities were normalized by the highest intensity band. After preprocessing, PCA was performed in the region 200-1700 cm^{-1} for two parts of seed (cotyledons and perisperm) and two quinoa genotypes (Puno and Titicaca). The spectra preprocessing was realized using the Spectragryph software (Menges, 2018) while PCA analysis was performed using the PAST software (Hammer et al., 2001). In general, principal components are composed of scores and loadings. When using PCA analysis, it is possible to make data visualization and to simultaneously reduce data size, allowing segregation between classes. In other words, the scores and loadings reveal the differences between the samples.

3. Results and discussion

3.1. The quinoa fruit

The quinoa fruit, at the anatomical level, comprises pericarp covering seed. The fruit of quinoa in an achene covered by perigonium. The outer layer of the fruit, consisting of one seed, is the pericarp. The perisperm is the storage organ of quinoa seeds (Jacobsen and Stølen, 1993). The quinoa fruit achene (1–2.6 mm in diameter) is round, flattened, and oval-shaped, with its basic colors ranging from yellow to pink (Fig. 1A–D), which most likely depends on the phase of maturity (Valcárcel-Yamani and Lannes, 2012).

As seen in the fruit's longitudinal section (Fig. 2 A, B), the pericarp is formed from two layers, easily detached from the seed coat. The outer pericarp cells are large and papillose, while a secondary discontinuous layer is composed of a tangentially stretched cell (Prego et al., 1998). The remaining structures below the pericarp represent the seed compartments.

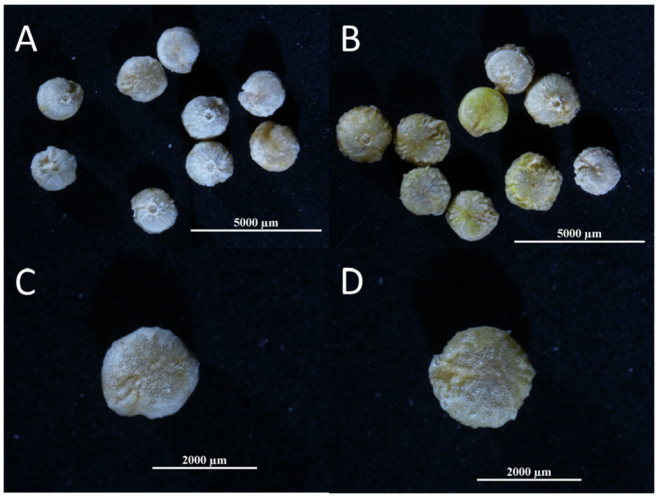

Fig. 1. Stereomicroscope micrographs of achene apical and basal pole of two quinoa genotypes Puno (A, C) and Titicaca (B, D) after harvesting. Magnification was up to 20x.

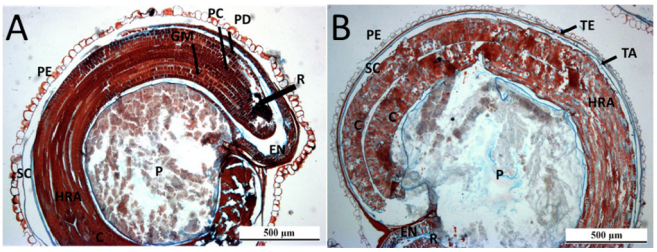

Fig. 2. Light microscopy of a median longitudinal section of the *Chenopodium quinoa* fruit, for Puno (A) and Titicaca (B) genotypes. Pericarp (PE), seed coat (SC), two cotyledons (C), Hypocotyl Radicle Axis (HRA), Endosperm (EN), perisperm (P), radicle or root cup (R), Testa (TE), Tapetum (TA), Protoderem (PD), Ground meristem (GM), Procambium (PC). Sections were stained with safranin and alcian blue and observed at 5 times magnification.

3.2. The quinoa seed

The seed coat is smooth and thin, consisting of two cell layers (Fig. 2A and B): the testa and the integumentary tapetum, both presented by dry cells without cell content (Sukhorukov and Zhang, 2013). In the quinoa seed (Fig. 2 A, B), the embryo or germ is campylotropous, surrounding the starch-rich perisperm like a ring, and together with the seed coat, they represent the bran fraction, which is relatively rich in fat and protein (Valcárcel-Yamani and Caetano da Silva Lannes, 2012). The embryo consists of a hypocotyl-radicle axis (Fig. 2A and B) and two cotyledons (Fig. 2B), though lacking a leaf primordia. In the axis, both the root apical meristem with the root cap and the shoot apical meristem are differentiated. The shoot apical meristem forms a conical structure between the two cotyledons. Protoderm, ground meristem and procambium are visible in the axis and cotyledons. The endosperm of the mature seed consists only of two cell layers around the radicule, enveloping the hypocotyl-radicle axis of the embryo (Fig. 2A). The perisperm consists of large and thin-walled cells, mostly uniform in shape (Fig. 2A and B), completely full of starch grains, morphologically similar to the grass starchy endosperm (López-Fernández and Maldonado, 2013).

3.3. Raman signature of main storage seed reserves

Fig. 3 shows the characterization of the quinoa seed by Raman microspectroscopy. The Raman spectra of quinoa seeds show predominant bands of polysaccharides and proteins arising from vibrations of the C–H, C=O, C–N, N–H. The major Raman scattered bands of polysaccharides in the perisperm were recorded in the range from 200

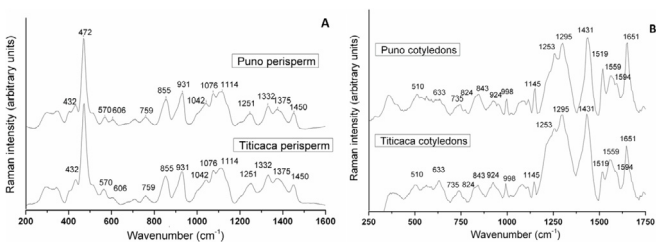

Fig. 3. Raman spectra of the quinoa seed recorded at perisperm (A) and cotyledon position (B). The most intensive peak at 472 cm^{-1} refers to starch (A), 1431 cm^{-1} and 1651 cm^{-1} refers to amino acid tryptophan and Amide I group (B), respectively.

to 1600 cm^{-1} (Fig. 3A), and are in line with previously published results from histochemical analysis of *Ch. quinoa* seeds (Prego et al., 1998) where there was not any indication of protein fraction occurrence in the perisperm. The region between 800 and 1500 cm^{-1} (Fig. 3A) provided a complex of exact band assignments to polysaccharides, because the vibrations of glucose molecules dominate in that spectral region, and consequently starch exhibits characteristic spectral vibrations (Kizil et al., 2002). The region between 1200 and 1500 cm^{-1} mainly shows the bands from basic structural compounds, including several bands originated from carbohydrates. For instance, the band at 1450 cm^{-1} (Fig. 3A) corresponds to CH_2 bending modes. The region between 1200 and 1340 cm^{-1} presents the contributions of several vibrational modes (Fig. 3A), such as medium intensity bands at 1332 and 1251 cm^{-1} (assignment to C–O, C–O–H stretching and C–C–H, C–O–H deformations) (Almeida et al., 2010). In the spectral region between 800 and 1200 cm^{-1}, the positions of the C–O, C–C and C–H stretching are assigned to 1114, 1076, 1042, 855 cm^{-1} and C–O–C deformation modes of R-1,4 glycosidic linkages in starches at 931 cm^{-1} (Kizil et al., 2002). That region is also known as the "fingerprint" for carbohydrates, containing the majority of the Raman bands used for unique identification of the sample (Kizil et al., 2002). Vibrations in the 400–800 cm^{-1} spectral region are in general due to C–C–O and C–C–C deformations, which are related to the glycosidic ring skeletal deformations. The most specific and highly intense Raman band at 472 cm^{-1} has been used as a marker to identify the presence of starch in different samples, as well as to characterize the pyranose ring in glucose of amylose and amylopectin, with low intensity bands at 432, 759, and 1375 cm^{-1}, as constituents of starch. In this study, low intensity bands at 570 and 606 cm^{-1} represent starches (Fig. 3A), and can be also attributed to the skeletal modes of the pyranose ring (Almeida et al., 2010). The starch composition of the quinoa perisperm was previously described by Varriano Marston and DeFrancisco (1984). Since the perisperm cells are full of angular-shaped starch grains, Prego et al. (1998) have indicated that quinoa seed starch mainly contains amylopectin.

It was found that the second type of Raman spectra of the *Ch. quinoa* seed corresponded to the protein content located at the embryonic region (Fig. 3B). This is also in agreement with results of the histochemical analysis of this seed region (Prego et al., 1998). The protein components are primarily represented by a spectrum of globulin as the main quinoa protein, with three characteristic signal regions of Amide I, II, and III. The typical Raman spectrum of quinoa seed protein shows C═O stretching vibration and N–H wagging in the peptide bonds coming from Amide I group at 1651 cm^{-1}. The Amide II and III broad bands are centered near 1559 and 1295 cm^{-1} (Fig. 3B), and they are due to N–H bend and C–N stretching vibration, respectively. The line at 924 cm^{-1} can be assigned to amino acid proline as well as low intensity bands at 633 cm^{-1}, with doublets at 824 and 843 cm^{-1} (Schulmerich et al., 2013). According to Stikic et al. (2012), the seed of the Puno cultivar has higher contents of proline and alanine. The band at 1253 cm^{-1} could indicate the presence of tyrosine while the band at 1519 cm^{-1} is consistent with the peak for glutaminic acid as a amino acids present in quinoa globulin (Zhu et al., 2011; Lee et al., 2013). In addition, the broad peak near 1431 cm^{-1} could be due to amino acid tryptophan, namely, the band is assignable to indole aromatic ring stretching (Zhu et al., 2011). A sharp and low intensity band at 998 cm^{-1} position is assigned to aromatic ring vibration (Fig. 3B), which arises from C–C symmetric ring breathing of phenylalanine amino acid residues (Lee et al., 2013). Also, some studies (Kolozsvari et al., 2015) described the presence of phytin globoids by the band at about 1000 cm^{-1}. Konishi et al. (2004) have already described phytin as a major component of protein bodies inside the quinoa embryonic cells.

The Raman spectrum in the 500-540 cm^{-1} spectral region could indicate the presence of quinoa globulin and the Raman band at 510 cm^{-1} correspond to the most preferred conformations of the bonds

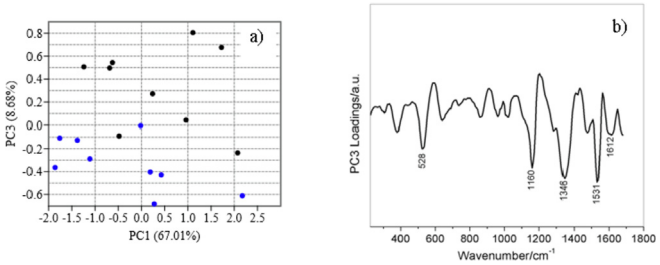

Fig. 4. a) Score plot of the first principal component (PC1) *versus* the third principal component (PC3) of the Puno quinoa cotyledons (blue cycle) and Titicaca quinoa cotyledons (black cycles); b) Loading plot corresponding to PC3.

(gauche-gauche-gauche/trans) in many naturally occurring proteins with disulphide (S–S) bridges (Schulz and Baranska, 2007). A similar observation was reported in the study of rice globulins with Raman spectroscopy, where the results revealed the high amount of sulfur containing amino acids such as cysteine or methionine, as constituents of globulins (Ellepola et al., 2006).

3.4. PCA of the Raman spectra recorded from quinoa cotyledon and perisperm

Multivariate analysis, based on PCA, was applied in order to differentiate between the quinoa genotypes. Fig. 4 presents the scores and loadings plots of the PCA for characteristic spectral region. The PCA analysis was performed using 9 samples of cotyledon and 8 samples of perisperm for each genotype.

The score plot of PC1 *versus* PC3 (Fig. 4a) shows a reasonably good separation between the samples.

The loading plot of the PC3 (Fig. 4b) displays the peaks that separate the Puno quinoa cotyledon from the Titicaca quinoa cotyledons.

As can be seen, the bands such as those in the spectral range 1200-1700 cm^{-1} are primarily assigned to the protein structure (e.g. Amide I and Amide II) and some specific amino acids (e.g. glutaminic acid) according to Zhu et al. (2011). These results indicate that differences between our genotypes are based on protein structural properties. The differences between investigated genotypes may be explained by their chemical composition. However, Aluwi et al. (2017) have compared Puno and Titicaca cultivars and found similar percentages of proteins (14.7 and 14.4%, respectively). Our results also did not show significantly different values in protein content between the seeds of Puno (14.1%) and Titicaca (14.0%). Fig. 5a highlights the relatively good separation of perisperm samples from two genotypes into two different groups, where the first and third principal components described ~78.5% of data variance.

The peaks, which are mainly responsible for this differentiation, can be observed in Fig. 5b. In the spectral range from 460 to about 600 cm^{-1}, the most important peaks for genotypes separation at

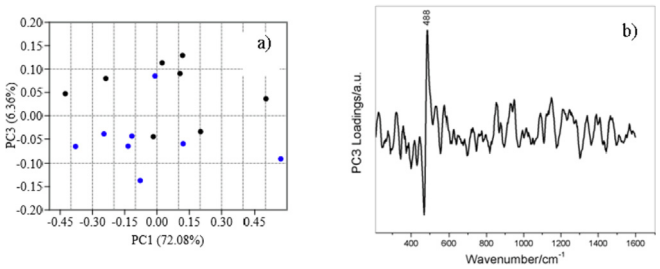

Fig. 5. A ccore plot of the first principal component (PC1) *versus* the third principal component (PC3) of the Puno quinoa perisperm (blue cycle) and Titicaca quinoa perisperm (black cycles); b) A loading plot corresponding to PC3.

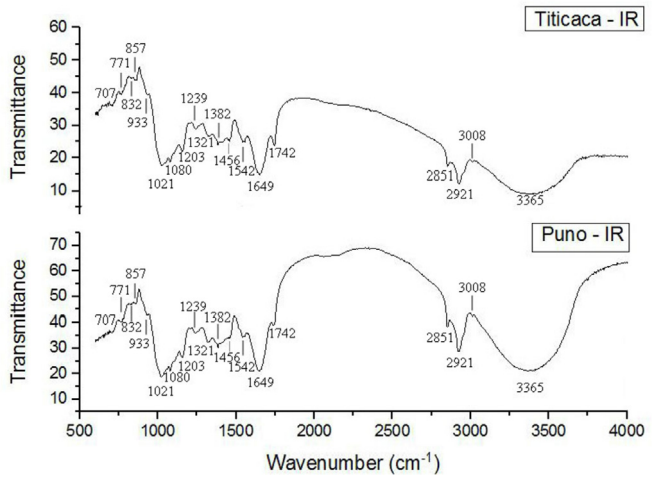

Fig. 6. Infrared spectra of ground quinoa seeds of two genotypes (Titicaca and Puno).

perisperm region can be detected. The peaks are mainly responsible for the differentiation of perisperm of the Titicaca cultivar compared to the perisperm of the Puno cultivar. That spectral region involves the deformation modes of the C—C—O and C—C—C deformations, as a marker for identifying the presence of starch. According to Aluwi et al. (2017), a higher percentage of quinoa seed starches was detected in Puno (62.6%) than in Titicaca (56.4%). In general, as for the Titicaca cultivar, the total carbohydrate represents the main seed component at approximately 54–57%, according to the study of Pulvento et al. (2012). The main carbohydrate component of quinoa is a starch and in our research the seeds of Titicaca and Puno contained similar starch content (54.1 and 55.6%, respectively). The identified peaks in our study peaks may be assigned to the pyranose ring of amylose, or predominantly amylopectin as specific for quinoa (Prego et al., 1998). As previously discussed by Almeida et al. (2010), the bands in the region 430-490 cm^{-1} are related to the evaluation of the amylose and amylopectin concentration present in the starchy samples.

3.5. FT-IR of quinoa seed

There was no distinction in the IR spectra between the two analyzed genotypes and main peaks, as presented in Fig. 6.

The band at 3365 cm^{-1} is assigned to the O—H stretching vibrations. Peaks at 3008 and 2921 cm^{-1} are due to C—H bonds, while the peak at 2851 cm^{-1} is assigned to the CH_2 and CH_3 groups from aldehydes/ketones (Garcia-Salcedo et al., 2018). The band at 1741 cm^{-1} is a result of C═O carbonyl stretching, while the 1648 cm^{-1} band may be assigned to the amide region of the proteins (Rossell, 2013). The observed alcohol and carbonyl stretching could be assigned to the chemical structure of quinoa saponins (Soliz-Guerrero et al., 2002). Those two peaks and the peak registered at 1542 cm^{-1} are particularly important since they represent protein amino acids and can reveal modifications in the secondary structure of proteins (Garcia-Salcedo et al., 2018). The band at 1080 cm^{-1} can be attributed to the pyranose structure of CH, while the 1021 cm^{-1} band can be assigned to the C—H bending from aromatic structures, which is also recorded in certain previous studies (Abugoch et al., 2011). Different substitutions in aromatic rings can be detected in the fingerprint region, characterized by aromatic C—H out-of-plane bend (857, 831, 771, 706 and 687 cm^{-1}).

4. Conclusions

This study confirmed the successful application of Raman spectroscopy in the detection of proteins and polysaccharides of quinoa seed storage reserves, and in a straightforward and fast manner. The assessment of the scores of the principal components based on the Raman spectra revealed two groups in both seed parts (cotyledons and perisperm). The analysis of the loadings highlighted the band at 472 cm^{-1}, presumably related to the amylopectin content in perisperm, as compound which contributes to the differences between the genotypes. Regarding the spectra recorded at the cotyledons part, the highest loadings derived from Amide I, II and quinoa protein with globoid crystals were responsible for the genotype separation. These results indicate that Raman spectroscopy is very useful method for localisation, quantification and structural identification of stored reserves inside the seeds of different genotypes of quinoa. IR analysis, similar to the measurements of the crude proteins and starch contents in the seeds, showed no differences in biochemical composition of seeds of two analyzed genotypes.

Conflicts of interest

None.

Acknowledgements

Authors acknowledge the financial support of the Projects of the Serbian Ministry of Education, Science and Technological Development (TR31005, ON171032), as well as the support of Mr. Radenko Radošević from the Faculty of Agriculture, University of Belgrade, for the technical help in preparing the microslides.

References

Abugoch, L.E., Tapia, C., Villaman, M.C., Yazdani-Pedram, M., Diaz-Dosque, M., 2011. Characterization of quinoa proteinechitosan blend edible films. Food Hidrocolloids 25, 879–886. https://doi.org/10.1016/j.foodhyd.2010.08.008.

Almeida, M.R., Alves, R.S., Nascimbem, L.B., Stephani, R., Poppi, R.J., de Oliveira, L.F., 2010. Determination of amylose content in starch using Raman spectroscopy and multivariate calibration analysis. Anal. Bioanal. Chem. 397 (7), 2693–2701. https://doi.org/10.1007/s00216-010-3566-2.

Aluwi, N.A., Murphy, K.M., Ganjyal, G.M., 2017. Physicochemical characterization of 28 different varieties of Quinoa. Cereal Chem. 94 (5), 847–856. https://doi.org/10.1094/CCHEM-10-16-0251-R.

Ellepola, S.W., Choi, S.M., Phillips, D.L., Ma, C.Y., 2006. Raman spectroscopic study of rice globulin. Cereal Sci. 43, 85–93. https://doi.org/10.1016/j.jcs.2005.06.006.

Encina-Zelada, C., Cadavez, V., Pereda, J., Gomez-Pando, L., Salva-Ruiz, B., Teixeira, J.A., Ibanez, M., Liland, K.H., Gonzales-Barron, U., 2017. Estimation of composition of quinoa (*Chenopodium quinoa* Willd.) grains by Near-Infrared Transmission spectroscopy. LWT- Food, Sci. Technol. 79, 126–134. https://doi.org/10.1016/j.lwt.2017.01.026.

Garcia-Salcedo, A.J., Torres-Vargas, O.L., Ariza-Calderon, H., 2018. Physical-chemical characterization of quinoa (*Chenopodium quinoa* Willd.), amaranth (*Amaranthus caudatus* L.), and chia (*Salvia hispanica* L.) flours and seeds. Acta Agron. 67 (2), 215–222. https://doi.org/10.15446/acag.v67n2.63666.

Gordillo-Bastidas, E., Díaz-Rizzolo, D.A., Roura, E., Massanés, T., 2016. Quinoa (*Chenopodium quinoa* Willd), from nutritional value to potential health benefits: an integrative review. J. Nutr. Food Sci. 6 (3), 1–10. https://doi.org/10.4172/2155-9600.1000497.

Hammer, Ø., Harper, D.A.T., Ryan, P.D., 2001. PAST: paleontological statistics software package for education and data analysis. Palaeontol. Electron. 4 (1), 9pp. http://palaeo-electronica.org/2001_1/past/issue1_01.htm.

ISO (International Organization for Standardization) 10520, 1997. Native Starch - Determination of Starch Content - Ewers Polarimetric Method. (en).

Jacobsen, S.-E., Muica, A., 2002. Genetic resources and breeding of the Andean grain crop quinoa (*Chenopodium quinoa* Willd.). Plant Genet. Resour. Newsl. 130, 54–61.

Jacobsen, S.-E., Stølen, O., 1993. Quinoa-morphology and phenology and prospects for its production as a new crop in. Eur. J. Agron. 2, 19–29.

Kizil, R., Irudayaraj, J., Seetharaman, K., 2002. Characterization of irradiated starches by using FT-Raman and FTIR spectroscopy. J. Agric. Food Chem. 50 (14), 3912–3918. https://doi.org/10.1021/jf011652p.

Kolozsvari, B., Firth, S., Saiardi, A., 2015. Raman spectroscopy detection of phytic acid in plant seeds reveals the absence of inorganic polyphosphate. Mol. Plant 8 (5), 826–828. https://doi.org/10.1016/j.molp.2015.01.015.

Konishi, Y., Hirano, S., Tsuboi, H., Wada, M., 2004. Distribution of minerals in quinoa (*Chenopodium quinoa* Willd.) seeds. Biosc. Biotech. Biochem. 68 (1), 231–234. https://doi.org/10.1271/bbb.68.231.

Lee, H., Cho, B.C., Kim, M.S., Lee, W.H., Tewari, J., Bae, H., Sohn, S.I., Chi, H.Y., 2013. Prediction of crude protein and oil content of soybeans using Raman spectroscopy. Sensor. Actuator. B Chem. 85, 694–700.

López-Fernández, M.P., Maldonado, S., 2013. Programmed cell death during quinoa perisperm development. J. Exp. Bot. 64 (11), 3313–3325. https://doi.org/10.1093/

jxb/ert170.
Menges, F., 2018. Spectragryph - Optical Spectroscopy Software. Version 1.2.8, 2018. http://www.effemm2.de/spectragryph/.
Noulas, C., Karyotis, T., Iliadis, C., 2015. GREECE (Chapter 6).1.6 In: FAO & CIRAD. State of the Art Report of Quinoa in the World in 2013, pp. 492–510 (Rome).
Prego, I., Maldonado, S., Otegui, M., 1998. Seed structure and localization of reserves in *Chenopodium quinoa*. Ann. Bot. 82, 481–488. https://doi.org/10.1006/anbo.1998.0704.
Pulvento, C., Riccardia, M., Biondib, S., Orsinic, F., Jacobsen, S.E., Ragabe, R., Lavinia, A., 2015. Quinoa in Italy: research and perspectives (Chapter 6).1.3 In: FAO & CIRAD. State of the Art Report of Quinoa in the World in 2013, pp. 454–465 (Rome).
Pulvento, C., Riccardi, M., Lavini, A., Iafelice, G., Marconi, E., d'Andria, R., 2012. Yield and quality characteristics of Quinoa grown in open field under different saline and non-saline irrigation regimes. J. Agron. Crop Sci. 198, 254–263. https://doi.org/10.1111/j.1439-037X.2012.00509.x.
Rossell, C.A., 2013. Authentication of Andean Flours Using a Benchtop FT-IR System and a Portable FT-IR Spectrometer. Master Thesis. Graduate Program in Food Science and Technology, The Ohio State University, USA.
Schulmerich, M.V., Gelber, M.K., Azam, H.M., Harrison, S.K., McKinney, J., Thompson, D., Owen, B., Kull, L.S., Bhargava, R., 2013. Amino acid quantification in bulk soybeans by transmission Raman spectroscopy. Anal. Chem. 85 (23), 11376–11381. https://doi.org/10.1021/ac402284b.
Schulz, H., Baranska, M., 2007. Identification and quantification of valuable plant substances by IR and Raman spectroscopy. Vib. Spectrosc. 43, 13–25. https://doi.org/10.1016/j.vibspec.2006.06.001.
Soliz-Guerrero, J.B., Jasso de Rodriguez, D., Rodriguez-Garcia, R., Angulo-Sanches, J.L., Mendez-Padilla, G., 2002. Quinoa saponins: concentration and composition analysis. In: Janick, J., Whipkey, A. (Eds.), Trends in New Crops and New Uses. ASHS Press, Alexandria, VA, pp. 110–114.
Stikic, R., Glamoclija, Dj, Demin, M., Vucelic-Radovic, B., Jovanovic, Z., Milojkovic-Opsenica, D., Jacobsen, S.E., Milovanovic, M., 2012. Agronomical and nutritional evaluation of quinoa seeds (*Chenopodium quinoa* Willd.) as an ingredient in bread formulations. J. Cereal. Sci. 55, 132–138. https://doi.org/10.1016/j.jcs.2011.10.010.
Sukhorukov, A.P., Zhang, M., 2013. Fruit and seed anatomy of *Chenopodium* and related genera (*chenopodioideae, chenopodiaceae/amaranthaceae*): implications for evolution and taxonomy. PLoS One 8 (4), e61906. https://doi.org/10.1371/journal.pone.0061906.
Valcárcel-Yamani, B., Lannes, S.C.S., 2012. Applications of quinoa (*Chenopodium quinoa* Willd.) and amaranth (*Amaranthus spp.*) and their influence in the nutritional value of cereal based foods. Food Public Health 2 (6), 265–275. https://doi.org/10.5923/j.fph.20120206.12.
Valencia-Chamorro, S.A., 2003. Quinoa. In: Caballero, B. (Ed.), Encyclopedia of Food Science and Nutrition 8. Academic Press, Amsterdam, pp. 4895–4902.
Varriano-Marston, E., DeFrancisco, A., 1984. Ultrastructure of quinoa fruit (*Chenopodium quinoa* Willd.). J. Food Microst. 3 (2), 165–173. http://digitalcommons.usu.edu/foodmicrostructure/vol3/iss2/9.
Zhu, G., Zhu, X., Fan, Q., Wan, X., 2011. Raman spectra of amino acids and their aqueous solutions. Spectrochim. Spectrochim. Acta Part A: Mol. Biomol. Spectrosc. 78, 1187–1195. https://doi.org/10.1016/j.saa.2010.12.079.